

Optical/infrared observations of high-redshift galaxy clusters

H. K. C. Yee

Department of Astronomy and Astrophysics, University of Toronto, Toronto, Ontario, M5S 3H8, Canada email: hyee@astro.utoronto.ca

Abstract. Galaxy clusters at $z \sim 1$ are particularly important in the study of cluster evolution and the application of clusters to cosmological studies. We briefly discuss the difficulties in creating well-defined, large, high-redshift cluster samples, and some of the techniques used in optical/IR imaging to overcome them. We give a summary of the current state of optical/IR observations of the relatively small number of high-redshift clusters identified so far, including discussions of the galaxy luminosity function, the Fundamental Plane, the color-magnitude relation, and the Butcher-Oemler effect. The application of photometric redshift techniques is also highlighted.

1. Introduction

Galaxy clusters, being the largest mass concentrations in the Universe, have long played an important role in both the study of galaxy evolution and the determination of cosmological parameters. In the former, galaxy clusters offer a unique laboratory for investigating the relationship between galaxy formation and evolution and the environment; in the latter, the mass-to-light ratio and the evolution of the mass function of clusters allow us to measure the mass density parameter Ω_m , the amplitude of the perturbation spectrum σ_8 (e.g., Oukbir & Blanchard 1992), and the dark matter equation of state w (e.g., Levine et al. 2002, and many others). In both cases, the leverage and advantage offered by having a sample with a large redshift coverage are significant. In the case of cluster evolution, at the redshift of ~ 1 we are approaching the formation epoch of clusters, often put at $z \sim 2$ to 5, so that we would be in a much better position to observe the evolutionary effects. For the determination of cosmological parameters, a large baseline of redshift allows us to measure the evolution of the mass function, breaking the degeneracy between Ω_m and σ_8 . The measurement of the mass function at $z \sim 1$ of a sufficiently large sample will also provide a chance to constrain w . However, the number of known high-redshift galaxy clusters, even just at $z > 0.8$, remains small, and these very often were found either as the tail of the distribution of a systematic survey, or by serendipity.

In this review we will examine the roles of optical/IR observations in the study of high-redshift galaxy clusters. (I will limit high-redshift to mean $z > 0.8$.) We will first address the important issue of defining a useful sample of clusters at high redshifts, specifically finding clusters using optical/IR imaging (Section 1). We then examine the still relatively small amount of current observations of clusters at $z \sim 1$. Section 3 focuses on imaging observations. This includes discussions of the cluster galaxy luminosity function, the Fundamental Plane of early-type galaxies, the color-magnitude relation, and the Butcher-Oemler effect. A brief discussion of spectroscopy and the application of photometric redshift techniques to high-redshift clusters is presented in Section 4. We end with a brief look at the future prospects of optical/IR observations of $z \sim 1$ clusters.

2. The search for high-redshift clusters

As recent as five or six years ago, the number of $z > 0.8$ clusters was on the order of a dozen. Most of these were found as the high-redshift tail of the distribution from X-ray surveys. A few were discovered by their association with $z \sim 1$ radio galaxies. The difficulty in finding high-redshift clusters is due to separate problems in the two major methods of finding clusters. For X-ray surveys, the available instruments simply do not go deep enough and cover sufficient areas. Rosati et al. (2002) provide a summary of the state of $z \sim 1$ clusters selected by X-ray observations as of a couple of years ago. For the more classical optical imaging surveys, the increased column of foreground galaxies presents a daunting problem of projection contamination which increases with redshift. Postman et al. (1996) used the so-called match-filter technique to optimize the identification of enhanced density clumps of galaxies that have the properties expected of clusters. Gonzalez et al. (2003) use an ingenious method of measuring background light fluctuations from shallow images from a small telescope as markers for possible high redshift over-density regions. However, these attempts to use optical imaging to search for high-redshift clusters suffer a typical contamination rate of ~ 25 to 30%.

Gladders & Yee (2000) proposed a method of using two-filter optical imaging to search for high-redshift clusters to overcome the projection problem. This technique uses the observation that the cores of clusters are dominated by early-type galaxies which follow the well-known color-magnitude relation. Thus, by searching for galaxy density enhancements in successive slices of colors, one can effectively isolate early-type galaxies at different redshift intervals, removing the projection problem if the proper filters are chosen. The recent arrival of large mosaic CCD cameras on 4m-class telescopes also matches the depth and areal coverage required for meaningful high-redshift cluster searches.

The Red-Sequence Cluster Survey (RCS) is a 92 square degree imaging survey designed to optimize the detection of galaxy clusters with $0.5 < z < 1.2$, exploiting these recent developments. The survey, conducted with the CFHT 12k and CTIO Mosaic 8k cameras, obtained images in z' and R_C filters, which straddle the 4000Å break for early-type galaxies at $0.45 < z < 1.3$. The survey technique is very successful at identifying clusters at redshifts up to ~ 1 . The redshift distributions of clusters for different richness bins from the first catalogs of ~ 10 square degrees (Gladders & Yee 2004) are shown in Figure 1. Spectroscopic confirmations of over 60 clusters with redshifts from 0.2 to 1.1 have been obtained. Blindert et al. (2004, these proceedings) show velocity histograms for seventeen $0.2 < z < 0.65$ clusters, demonstrating that all but one (which has poor data) are consistent with significant clumps in velocity space. Extrapolating from the well-analysed 10 square degrees from Gladders & Yee (2004), we can expect the order of 350 clusters of richness Abell 0 and higher at redshift between 0.8 and 1.2 to be found in the RCS, greatly expanding the number of known $z \sim 1$ clusters.

The RCS demonstrates the efficiency of searching for clusters using the red-sequence as a marker of excess galaxy density. Similar techniques using a larger number of filters to search for clusters in multi-color/angular position phase space have also been developed for the lower redshift data of SDSS. With the commissioning of the MegaCam, a 36-CCD, one square degree field-of-view camera at the CFHT, we have begun the RCS2, a 1000 square degree optical cluster survey. This survey, modeled after the RCS but with somewhat shallower images in z' , r , and g , will discover approximately 30,000 clusters, with 1000's at $z \sim 1$. A main scientific goal is to measure the cluster mass function evolution with sufficient statistical accuracy to constrain w , the equation of state of dark energy (see, e.g., Levine et al. 2002). The RCS2 requires ~ 43 nights of telescope time, and is expected to be completed by the end of 2005.

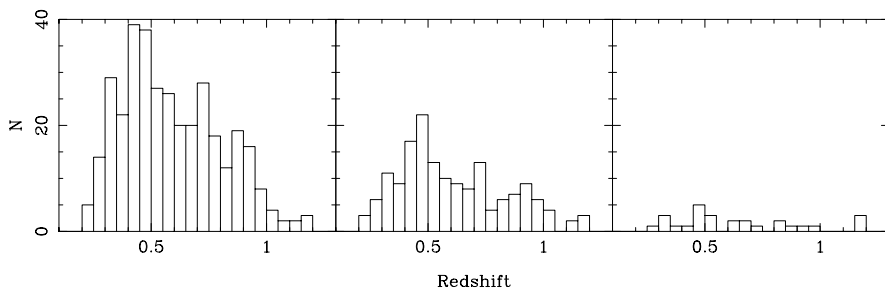


Figure 1. Redshift distributions of clusters in 9 sq deg of the RCS survey. The left panel shows the histogram for all clusters found; the middle panel, clusters with richness of approximately Abell 0 or greater ($\sigma_1 \gtrsim 500$ km/s); and the right panel, rich clusters of Abell 1 or richer ($\sigma_1 > 750$ km/s).

A major consideration, besides estimating the redshifts, in creating these large cluster surveys is to find a simple but robust means of characterizing the sample, which could number in the tens of thousands. The most significant attribute of a cluster is its mass, which is the parameter that allows the use of clusters for constraining cosmological parameters, and also for defining meaningful cluster samples for the study of cluster evolution. For these large samples, it is essential that some easily obtainable mass observables can be derived, preferentially from the survey data themselves. A number of recent studies showed that optical richness or total light does trace other more traditional mass estimators, such as velocity dispersion and X-ray temperature (e.g., Yee & Ellingson 2003; Bachall et al. 2003). Using robust calibrations of such relations between optical/IR properties and the more traditional mass observables over a large redshift range is likely the most promising (certainly the least expensive) method for estimating the mass function for the very large cluster surveys that are being carried out or planned.

3. Optical/IR imaging

3.1. Cluster galaxy luminosity function

Despite the disadvantage of being a relatively limited tool for understanding the evolution of galaxies, the luminosity function (LF) of cluster galaxies is probably the most easily measurable quantity for galaxy clusters. It can be estimated using simply direct images with statistical background corrections. However, the current information on the evolution of cluster galaxy LF is still rather limited, primarily due to the lack of substantial medium and high redshift cluster samples.

Most work on the LF of cluster galaxies is based on IR imaging, as at $z \sim 1$ the k -correction is less debilitating, compared to the optical bands. The LF in the IR also provide the most stable estimate of the stellar mass of the galaxies, which makes it more likely to be a reasonable proxy for measuring the mass function of clusters. This, however, is offset by the problems of much smaller field-of-view and less certain background count determination in K -band imaging (due to the difficulty in obtaining wide-area blank field counts). The largest compilation of K -band imaging of clusters covering a large redshift range is that of De Propriis et al. (1999). They reported K -band LFs for 38 clusters ranging in redshift from 0.14 to 0.92. However, there were only three clusters with $z > 0.8$, and five with $0.6 < z < 0.8$. They found that the K^* (the characteristic magnitude of a Schechter function fit) vs z relation is broadly consistent with passive evolution, and departs from no-evolution models at $z > 0.4$.

A few more papers on K -band LF have been published in the last few years, each dealing with a very small number (one to three) of clusters at $z \sim 1$, which nevertheless, still increase the sample at these redshifts by a significant factor. Ellis & Jones (2004) reported the LFs for three clusters at z between 0.8 and 1.0. Similarly, Kodama & Bower (2004) presented K -band LF for two clusters at somewhat higher redshifts, but based on clusters selected by their association with active galactic nuclei. Toft et al. (2003) measured the K -band LF for one $z = 1.0$ cluster. The primary conclusion from each of these studies is that the K^* 's derived extend the passive evolution interpretation of De Propris et al. to $z \sim 1.2$, consistent with a monolithic formation model with $z_f \sim 2$ to 3. These results are perhaps not surprising, as the LFs are all measured in essentially the cluster cores and the clusters in these investigations are all very massive, likely amongst the most massive clusters at these epochs.

3.2. The Fundamental Plane

The scaling relation of the Fundamental Plane (FP) for early-type galaxies provides the most stringent and robust constraints on the evolution of early-type galaxies. This is because the FP allows us to measure the mass-to-light ratio (M/L) of the galaxies. The FP relation requires measurements of the size, the surface brightness, and velocity dispersion of the galaxy, and hence is intrinsically much more difficult to derive for clusters at high-redshifts. Typically, morphological information has to be obtained using HST imaging, even at $z \sim 0.3$. The velocity dispersion measurement is a severe challenge at $z \sim 1$ even with 10m-class telescopes.

Given this difficulty, it is not surprising that the FP of less than a handful of clusters at $z > 0.5$ has been measured, all of which are X-ray luminous. MS1054-03, a very rich and extremely X-ray luminous cluster at $z = 0.83$, is the first cluster at high redshift in which the FP was established (van Dokkum et al. 1998); and Wuyts et al. (2004) extended the measurements to 22 galaxies. The measurements of the FP for three galaxies for the $z = 1.27$ cluster (RDCS J0848+4453) were obtained by van Dokkum & Stanford (2003). Of these three galaxies, one is an E+A galaxy and cannot be considered for FP. With only two galaxies, the tilt of the FP cannot be estimated, but nevertheless, the M/L values for these two galaxies can be estimated. Compared to the FP of Coma, these two galaxies are found to have a M/L_B a factor of ~ 4 smaller. The results from these clusters, combined with a few $z < 0.8$ clusters, are consistent with a passively evolving single burst stellar population of $z_f \sim 3$.

3.3. The color-magnitude relation

The color-magnitude relation (CMR) of early-type galaxies was recognized very early on as a key photometric property in galaxy clusters. The standard interpretation is that the CMR arises from differing metallicities in the formation process of galaxies of different masses (e.g., Arimoto & Yoshii 1987). The CMR offers three measurable quantities which can be used as diagnostics of galaxy formation and evolution in clusters: the color, the dispersion in color, and the slope (e.g., Bower et al. 1992; Stanford et al. 1998; Gladders et al. 1998).

Aragon-Salamanca et al. (1993) first presented the possible evolution of the CMR at high redshift, using K -band and optical imaging data for 10 clusters with $0.5 < z < 0.9$, showing that the color of the red-sequence at these redshifts is bluer than local clusters. The uniformity of the CMR observed led them to conclude that early-type galaxies in the cluster cores are coeval and homogeneous. Stanford et al. (1998) significantly reinforced these results by presenting a sample of 19 clusters with redshifts between 0.3 and 0.9, including using HST images to morphologically selected early-type galaxies for the CMR.

They found that the colors of the CMR have evolved only moderately compared to that of Coma, by about a rest frame $\Delta(U - J) \sim 0.5$, and that the slope and dispersion of the CMR at $z \sim 0.8$ are similar to lower z clusters. Subsequently, various authors added a small number of higher redshift clusters (e.g., van Dokkum et al. 2001; Blakeslee et al. 2003; Lidman et al. 2004). Holden et al. (2004) extended the redshift range of Stanford et al. (1998) using six clusters with HST images with redshifts between 0.78 and 1.27 with IR and optical photometry and HST morphologies, with the primary result that the last significant episode of star formation in early-type galaxies is likely at $z > 3$.

Gladders et al. (1998) demonstrated that the slope of the CMR can provide constraints on the formation epoch of early-type galaxies in clusters. Combining a sample of $z \sim 0.1$ Abell clusters and HST imaging of a few high-redshift clusters up to $z \sim 0.85$, they compared the measured slope to model slopes from Kodama & Arimoto (1997), and concluded that, at least for the relatively rich clusters at $z \sim 0.8$, their cores were formed at $z > 2.5$. However, the small sample at the higher redshifts clearly does not preclude a scatter of slope values which may arise from cluster cores having a variety of formation epochs and durations.

It should be noted that all the high-redshift clusters studied so far are basically the same set of about a dozen clusters at $z > 0.8$, and these are in general extremely rich or X-ray luminous clusters. More recently, Gladders et al. (2004, in preparation) examined the dispersion of the $i - K$ CMR from a large sample of RCS clusters at $z \sim 1$, with the intriguing preliminary result showing that the dispersion of the CMR appears to be larger for poorer clusters. If this result is confirmed, it would suggest that less massive clusters may have a more recent formation time, compared to the massive ones.

3.4. *The Butcher-Oemler effect*

The Butcher-Oemler (BO) effect (Butcher & Oemler 1984) was amongst the first observational evidence that galaxies evolve over cosmic time. The increase in the blue galaxy fraction (f_b) with redshift has been connected to the greater amounts of star formation in galaxies in higher-redshift clusters. It is increasingly clear that this higher blue fraction is primarily a reflection of the evolution of the infalling population (as opposed to the evolution of the CMR, which can be considered the “original” population more closely associated with the formation of the cluster core). In the simplest form the BO effect can be interpreted as the result of a combination of cosmologically driven changing galaxy infall rate and the truncation of star formation in the infalling galaxies (Ellingson et al. 2001), without reference to an evolving mechanism that turns galaxies red. However, despite two decades since its original discovery, both the magnitude (or existence) and the interpretation of the BO effect are still being debated vigorously.

Rakos & Schombert (1995) pushed the BO effect to $z \sim 0.9$ (with three clusters at $z > 0.8$) using photometry in the rest frame Stromgren filter system, and found that there is a general increase of f_b , from ~ 0.1 – 0.2 at low- z to as high as ~ 0.9 at $z \sim 0.9$. De Propriis et al. (2003) argued that a strong BO effect is not observed in the De Propriis et al. (1999) sample, when the cluster galaxies are selected by K -band magnitude, concluding that the BO effect mostly occurs in low-mass galaxies. However, it also appears that, based on their plots, one cannot rule out a BO effect for their sample. The f_b computed using a large subsample of RCS clusters with $0.4 < z < 1.2$ with z' -band selected galaxies inside r_{200} shows a general increase up to $f_b \sim 0.8$. The seemingly confusing and conflicting results from the many investigations in the BO effect likely arise from the very different operational definitions used to measure the blue fractions. For example, it is clear that the cluster-centric radius used to sample the galaxies greatly influences the results (e.g., see Ellingson et al. 2001). A dynamically defined radius such as

r_{200} , where one would sample galaxies in similar cluster dynamical state, would be a much more consistent way of selecting galaxies, compared to, say, a fixed metric radius (see, e.g., Yee 2003). Andreon et al. (2004) give an interesting discussion on the importance of the many aspects that impact on the measurement of the BO effect, including the magnitude limit, color-cut, cluster radius, and error estimation.

4. Spectroscopic observations

4.1. Spectroscopy

Spectroscopy of cluster galaxies provides two crucial sets of information: the redshifts – allowing membership information (though still not necessarily definitive) and dynamical analysis; and spectral features – providing much more detailed information on stellar populations than that from just colors. However, at $z \sim 1$, spectroscopic data with coverage and sample size similar to those at lower redshift is difficult and expensive. Currently, most $z > 0.8$ clusters have on the order of a dozen or fewer redshifts per cluster (with the exception of MS1054–03 with 30 redshifts, Wuyts et al. 2004). The EDisCS survey (Halliday et al., this conference) contains detailed spectroscopic studies of a set of $z \sim 0.7$ to 0.8 clusters. Spectroscopic data sets at $z \sim 1$ comparable to the moderate redshift ($0.2 < z < 0.6$) cluster samples of the CNOC1 (Yee et al. 1996) and the MORPH collaboration (Dressler et al. 1999) are still a few years away.

4.2. Very low-resolution spectroscopy: photometric redshift

The difficulties in obtaining spectroscopic data for a large sample of galaxies in high-redshift clusters make the application of photometric redshift techniques an attractive method for studying these clusters. Typical uncertainty of photometric redshifts is much larger than the velocity dispersion of a rich cluster; hence, photo- z 's can only be considered as a tool to limit the foreground and background contamination. Statistical background corrections based on a blank field galaxy sample with identical photo- z cuts are still needed. The application of photo- z techniques is especially beneficial for the study of the outskirts of clusters and high-redshift clusters. In both cases the relative ratio of the numbers of field and cluster galaxies is much larger. Using a photo- z sample of cluster galaxies should improve the derivation of the cluster galaxy LF and various analyses of galaxy populations based on photometric/color data. Furthermore, for high-redshift clusters, photo- z 's will greatly improve the efficiency of multi-object spectroscopy, especially in the outskirts of clusters, in that galaxies can be preselected for observation based on photo- z , greatly reducing the number of non-cluster spectra. A number of projects using photo- z techniques to select cluster members are discussed in these proceedings (e.g., Kodama et al., Nakata et al., Li et al.).

5. Future prospect and summary

The many results from different wavelength regimes indicate to us that galaxy clusters are intrinsically complex entities. They are intimately intertwined with their large scale environment, and the physical processes involved, from the outskirts to the core, are often complex and not subject to simple observations and analysis. Hence, to study the evolution of clusters, investigations using considerably larger samples (by more than an order of magnitude) than what have been done are essential to unravel the workings of these large aggregates of galaxies. The most robust preliminary conclusion about $z \sim 1$ clusters is that the core population of the rich clusters were likely formed at $z > 3$.

In the last few years there has been a general convergence of developments which will generate considerable advances and excitement in the study of high-redshift galaxy

clusters. Large and well-defined cluster surveys, in optical/IR, X-ray, and SZ-effect, are poised to produce significant $z \sim 1$ (and beyond) cluster samples. Instrumentation on 8–10m-class telescopes increasingly provide powerful tools to do detailed studies on these high-redshift clusters. An example is the wide-field multi-object spectrograph IMACS on the Magellan 6.5-m telescope, which offers the capability of obtaining up to 1000 spectra in a single observation. Similar capabilities are also being made available on the VLT, and the Keck and Subaru telescopes. The RCS has provided a large sample of clusters at $z > 0.8$ for which extensive spectroscopic, multi-color optical and IR-imaging are being carried out, along with some X-ray and SZ effect imaging. This, plus many projects being carried out at other large telescopes, will no doubt bring us closer to understanding the processes affecting the evolution of galaxy clusters.

Acknowledgements

I would like to thank my RCS collaborators. The RCS project is supported in part by operating grants from NSERC, from the University of Toronto, and from the Canada Research Chair Program.

References

- Andreon, S., Lobo, C., & Iovino, A. 2004 *MNRAS*, **349**, 889–898.
 Aragon-Salamanca, A., Ellis, R.S., Couch, W.J., & Carter, D. 1993 *MNRAS*, **262**, 764–794.
 Arimoto, N. & Yoshii, Y. 1987 *A.&A.* **173**, 23–38.
 Bachall, N., et al. 2003 *Ap.J.S.*, **148**, 243–273.
 Blakeslee, J.P. et al. 2004 *Ap.J.*, **599**, L143–L146.
 Bower, R., Lucey, J.R. & Ellis, R.S 1993 *MNRAS* **254**, 601–613.
 Butcher, H. & Oemler, A., Jr. 1984 *Ap.J.* **285**, 426–438.
 De Propris, R., Stanford, S.A., Eisenhardt, P.R., & Dickinson 2003 *Ap.J.* **598**, 20–35.
 De Propris, R., et al. 1999 *A.J.* **111**, 719–729.
 Dressler, A., et al. 1999 *Ap.J.S.* **122**, 51–80.
 Ellingson, E., Lin, H., Yee, H.K.C., & Carlberg, R.G 2001 *Ap.J.*, **547**, 609–622.
 Ellis, S.C. & Jones, L.R. 2004 *MNRAS*, **348**, 165–175.
 Gladders, M.D., Lopez-Cruz, O., Yee, H. K. C., & Kodama, T. 1998 *Ap.J.*, **501**, 571–577.
 Gladders, M.D. & Yee, H.K.C. 2000 *A.J.*, **120**, 2148–2162.
 Gladders, M.D. & Yee, H.K.C. 2004 *Ap.J.S.*, in press.
 Gonzalez, A.H., Zaritsky, D., Dalcanton, J.J., & Nelson, A. 2001 *Ap.J.S.* **137**, 117–138.
 Holden B.P., Stanford, S.A., Eisenhardt, P.R., & Dickinson M. 2003 *A.J.* **127**, 2484–2510.
 Kodama, T. & Arimoto, N. 1997 *A.&A.* **320**, 41–53.
 Kodama, T. & Bower, R. 2003 *MNRAS*, **346**, 1–12.
 Levine, E.S., Schulz, A.E., & White, M. 2002 *Ap.J.* **567**, 569–578.
 Lidman, C. et al. 2004 *A.&A.* **416**, 829–837.
 Oukbir, & Blanchard, A. 1992 *A.&A.* **262**, L21–L24.
 Rakos, K.D. & Schombert, J.M. 1995 *Ap.J.* **439**, 47–59.
 Rosati, P., Borgani, S., & Norman, C. 2002 *ARAA* **40**, 539–577.
 Stanford, S.A., Eisenhardt, P.R., & Dickinson M. 1998 *Ap.J.* **492**, 461–479.
 Postman, M., et al. 1996 *A.J.* **111**, 615–641.
 Toft, S., Soucaill, G., Hjorth, J. 2003 *MNRAS* **334**, 337–346.
 van Dokkum, P. & Stanford, S.A. 2001 *Ap.J.* **585**, 78–89.
 van Dokkum, P., Franx, M., Kelson, D.D., & Illingworth, G.D. 1998 *Ap.J.* **504**, L17–L21.
 van Dokkum, P. & Stanford, S.A. 2003 *Ap.J.* **585**, 78–89.
 Wuyts, S., van Dokkum, P., Kelson, D., Franx, M., & Illingworth, G. 2004 *Ap.J.* **604**, 677–688.
 Yee, H.K.C., & Ellingson, E. 2003 *Ap.J.*, **585**, 215–226.
 Yee, H.K.C., Ellingson, E., & Carlberg, R.G. 1996 *Ap.J.S.*, **102**, 269–287.
 Yee, H.K.C. 2003, *Astrophys. & Space Science*, **285**, 269–277.